Yugoslav Journal of Operations Research
3 (1993), Number 2, 199-218

APPLICATIONS OF NEURAL-NET COMPUTING TO TRANSIENT STABILITY ASSESSMENT AND ENHANCEMENT OF ELECTRIC POWER SYSTEMS

Miodrag ĐUKANOVIĆ

Nikola Tesla Institute
V.Hugo 3, 11000 Belgrade, Yugoslavia

Mirko MILIĆ

Faculty of Electrical Engineering, University of Belgrade
Bulevar Revolucije 73, 11000 Belgrade, Yugoslavia

Dejan J. ŠOBAJIĆ

Electric Power Research Institute, Power System Control
Palo Alto, CA 94304, USA

Yoh-Han PAO

Departments of Electrical Engineering and Computer Science,
Case Western Reserve University
Cleveland, Ohio 44106 USA

Abstract: This paper describes some application of artificial neural networks in electric power systems. The concept of adaptive pattern recognition and neural networks in the process of recognizing and classifying patterns is explained. The Generalized Delta Rule and the Functional Link Net architectures of neural nets and the unsupervised/supervised learning concept are discussed. Generalization capabilities of neural nets are illustrated in applications on unstable machine identification, calculation of voltage dips and calculation of generation shedding requirements.

Keywords: Short term system dynamics, transient stability, security assessment, neural-nets, adaptive pattern recognition

LIST OF SYMBOLS AND ABBREVIATIONS

n – the number of generator nodes;

P_{mi} – mechanical power of the i–th generator

$P_{ei}(0+)$ – electrical output (active power) of the i–the generator immediately after occurrence of a fault

E_i – electromotive force behind the transient reactance of the i–th generator

G_{ij}, B_{ij} – components of ij–th elements of the reduced short circuit admittance matrix for the network

$M_i = \frac{T_{Ji} S_{ni}}{w_s}$ – inertia constant of the i–th synchronous machine;

T_{Ji} – inertia time constant;

S_{ni} – rated apparent power;

w_s – synchronous speed of rotation;

$M_{\text{COI}} = \sum_{i=1}^{n} M_i$

δ_i – rotor angle of the i–th generator relative to the synchronously rotating reference frame

w_i – angular velocity of the rotor of the i–th generator relative to the synchronous velocity

$$\delta_0 = \frac{1}{M_T} \sum_{i=1}^{n} M_i \delta_i \quad ; \quad \theta_i = \delta_i - \delta_0 \quad ; \quad \tilde{w}_i = w_i - w_0$$

$$C_{ij} = E_i E_j B_{ij} \quad ; \quad D_{ij} = E_i E_j G_{ij} \quad ; \quad P_i = P_{mi} - E_i^2 G_{ii}$$

1. ARTIFICIAL NEURAL NETWORKS

Traditional pattern recognition techniques has been viewed as useful for recognizing and classifying objects that belong to different classes. However, existing conventional pattern recognition techniques are incapable of synthesizing complex and transparent mappings. They are computationally involved if applied in power systems, because a new discriminant function is required for any change in network topology or new disturbance location.

The addition of parallel distributed processing to traditional pattern recognition has given rise to a more powerful methodology, adaptive pattern recognition. The introduction of parallel distributed processing allows for adaptive learning and classification. Such subsymbolic–level processing seems to be appropriate for dealing with perception tasks and perhaps even with tasks that call for combined perception and cognition.

Artificial neural networks (ANN) [14] also known as parallel distributed processing systems, connectionist networks or adaptive systems are based upon the methods of information processing understood to exist in the brain. They consist of a large number of simple processing units, massively interconnected. Such processing architectures have capability to create its own sub-symbolic representation, to learn, to memorize, and to recall associatively. In the supervised learning of input/output pairs, the ANNs can predict accurately and generalize in the feature space. Neural systems are efficient in discovering similarities among large bodies of data and in synthesizing distributed fault-tolerant models for nonlinear, partly unknown and noise corrupted system.

A typical feedforward neural network is illustrated in Figure 1. A three layered network is shown, but in principle there could be more than one layer of internal representation units. The idea underlying the design of the network is that the information going to the input layer units are recoded into an internal representation and the outputs are generated by the internal representation rather than by the input pattern.

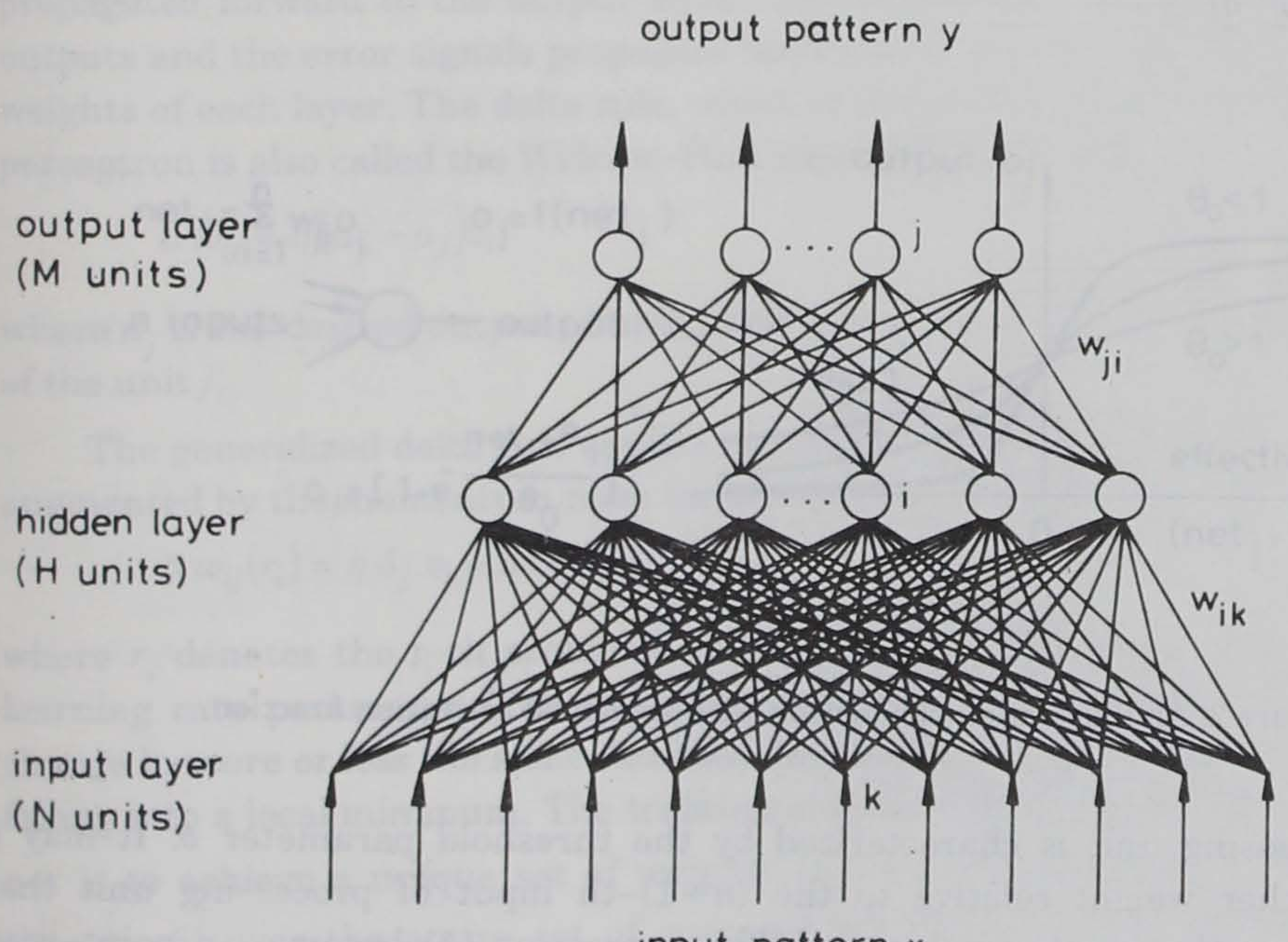

Figure 1. An illustration of feedforward neural network

Historically Rumelhart, Hinton and Williams demonstrated [17] that a feedforward layered machine of the Perceptron type with one or more internal layers could indeed train itself autonomously as desired if analytic functions were used for activation at the network nodes and if a generalized delta rule (GDR) was used to change the interconnecting weights, activation functions and thresholds until proper recognition capability had been attained. Supervised learning may be treated as a mechanism which when presented with a sequence of class labeled patterns learns an internal structure which allows it to generalize and to classify other patterns correctly. The input signals come either from the environment or from the outputs of other processing units and from the input pattern vector. A typical neuron, which is the elementary processor unit of a neural-net, utilizes the logistic activation function as shown in Figure 2. The parameter θ_j is called a threshold and determines the transition region of the function, while the parameter θ_0 determines the abruptness of the transition. Also shown is the weight corresponding to each unit, a collection of which forms the weight vector $\underline{w}$, where w_i represents the connection strength for the i-th input. The activation or total input for a unit in layer j is called $net_j = \sum^{n} w_{ji} o_i$.

The computation is typically performed by taking the scalar (dot) product of the input vector $\underline{w}$ and processing that value through an activation function f. In the vector notation:

$$o_j = f\left(\underline{w}^T \underline{o}\right) \tag{1}$$

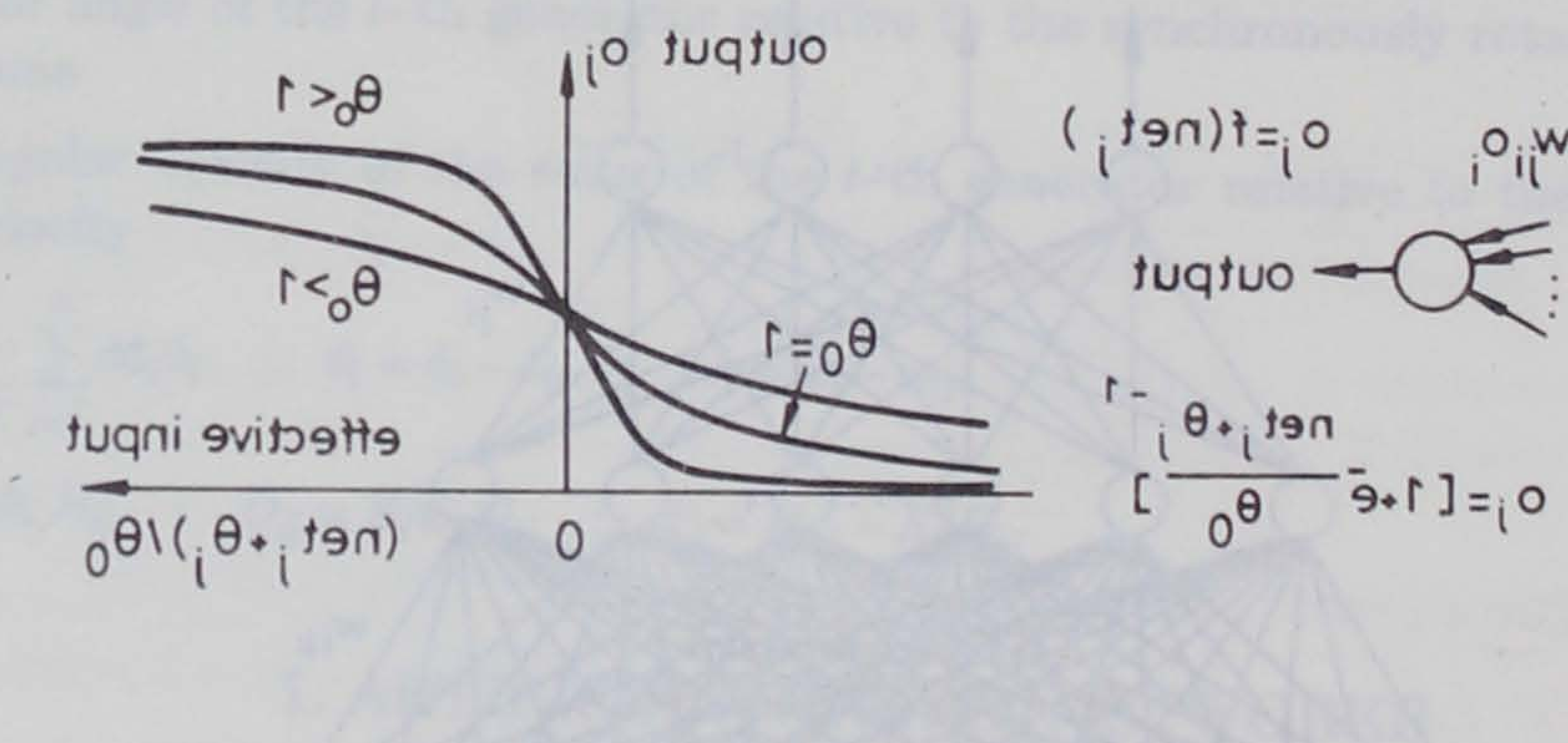

Figure 2. An illustration of a neuron with sigmoidal activation function

Each processing unit is characterized by the threshold parameter θ. It may be viewed as another weight relative to the $(n+1)$-th input of processing unit that receives permanently signal of value one. The expression (1) becomes in point-wise notation:

$$o_j = f\left(\sum_{i=1}^{n} w_{ji} o_i + \theta\right) \tag{2}$$

The activation function determines the output value of a processing unit. The sigmoidal activation function, that is a hybrid of the ramp and the step activation functions, shown in Figure 2, provides a graded nonlinear response to the input signal.

It has the equation:

$$f \stackrel{\Delta}{=} \frac{1}{1+e^{-\frac{net_j+\theta_j}{\theta_o}}} \tag{3}$$

The sigmoidal function has the important property of exponential maps that its first derivative can be expressed in terms of the function itself. This function yields an output which varies continuously from 0 to 1. The quantity θ_j serves as a "threshold" and positions the transition region of the f function.

In learning the hidden representation, that is, the weights and the threshold values, the network is presented with a pair of patterns, an input pattern and a corresponding desired output pattern. Using its (possibly incorrect) weights and thresholds, the network produces its own output pattern which is compared with the desired output pattern. The outputs of units in layer k are multiplied by various weights w_{ij} and these are inputs for the hidden layer $k+1$. Each node in a lower layer is connected to every node in the next layer without feedback connections from a higher layer to a lower layer. The input patterns are fed into the input layer and propagated forward to the output layer. The outputs are compared with the desired outputs and the error signals propagate backwards through the network adjusting the weights of each layer. The delta rule, which is the basis for training of the single-layer perceptron is also called the Widrow-Hoff rule and has the form:

$$\Delta w_{ij} = \eta\left(d_j - o_j\right)o_i \tag{4}$$

where d_j is the desired output of unit j and $\delta_j = d_j - o_j$ is the error signal at the output of the unit j.

The generalized delta rule applies to systems with hidden layers and is frequently augmented by the momentum term for convergence reasons, as:

$$\Delta w_{ij}(r_i) = \eta\, \delta_j\, o_i + \alpha\, \Delta w_{ij}(r_{i-1}) \tag{5}$$

where r_i denotes the i-th sequence of the iterative procedure, while η is called the learning rate parameter. The momentum term α tends to make the next weight-change in more or less the same direction as the last change keeping the network from falling into a local minimum. The training objective of the supervised learning neural-net is to achieve a unique set of weights ($\underline{w}$) and threshold ($\underline{\theta}$) that will minimize criteria (6) over the entire set of patterns (p). E is the sum of squared difference between the set of training outputs for all patterns p and the set of actual outputs.

$$E = 1/2 \sum_p \sum_k \left(d_k^{(p)} - o_k^{(p)} \right)^2 \tag{6}$$

A minimization is performed using a gradient-descent algorithm which always takes the steepest descending route down from the current position. Adjustment of weights are made first, updating the hidden-to output weights, computing so the δ_k's at the output layer and then back propagation these error signals to the hidden layer to compute δ_j's which with the input values are used to update the input-to hidden weights. Incorrect local minima can be recognized by failure to converge to the desired output pattern during the training process. In this case the gradient descent is started over again using new initial values for w_{ji} or new values for the learning rate η and the momentum term α.

Feedforward networks operate in two distinctive phases: learning phase and consulting phase. In the learning phase the patterns are fed into input layer and propagated forward to the output layer, where the actual outputs are compared with desired ones and the error is obtained. The error is propagated backwards through the network adjusting the weights of each layer. Adjustments of weights are made by first updating the hidden–to output weights, and computing the error signals at the output layer. Then, these terms are propagated back to the hidden layer to compute error signals which are used to update the input–to hidden weights.

This is schematically illustrated in Figure 3 where t_j is a desired output of unit j; δ_j is the error signal at the output of the unit j; η is the learning rate parameter; α is momentum term which determines the effect of past weights changes on the current direction of movement in weight space; m is the presentation number, net_j is the total input to a unit j; o_j is the output of a unit in layer j; f is a convenient logistic activation function.

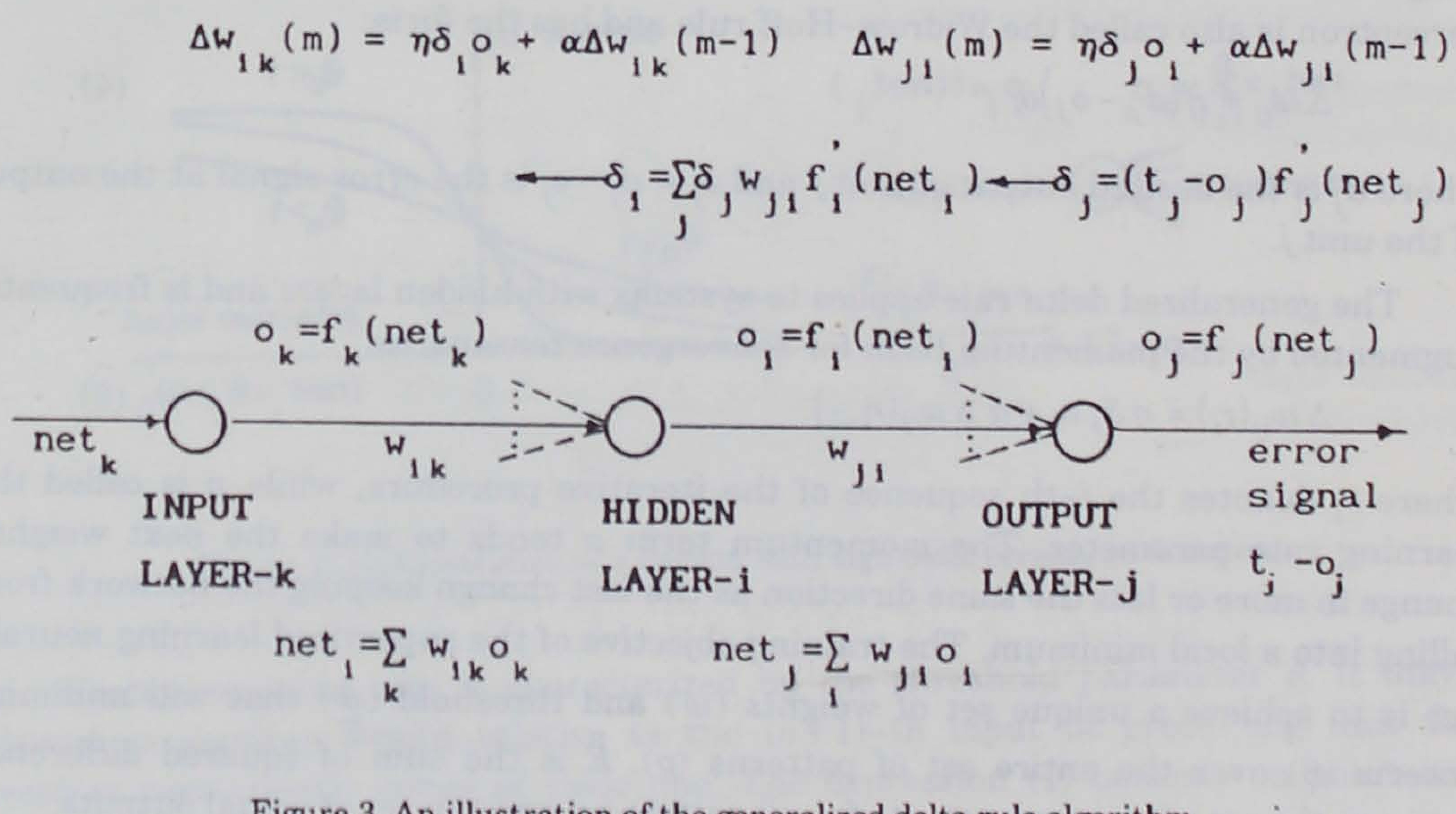

Figure 3. An illustration of the generalized delta rule algorithm

Functional Link Net (FLN) introduced by Pao [14] represents the new network architecture that allows unsupervised learning, supervised learning and associative retrieval to be carried out with the same net configuration and with the same data structure. The basic idea behind a Functional Link Net is the use of links for effecting nonlinear transformations of the input pattern before it is fed to the input layer of the actual network. In this way the generation of an enhanced pattern to be used in place of actual pattern is performed. There is mathematical basis, as well as pragmatic evidence that supervised learning can be achieved exceedingly well with a flat net and the delta rule if the enhancement are done correctly. This is in contrast to the conventional use of a net with the obligatory hidden layers and the generalized delta rule. No intrinsically new information is introduced, but the representation is enhanced. The flat architecture of the FLN exhibits highly desirable learning capabilities and in some applications drastically reduces the convergence time. In the functional expansion model, the FLN acts on each node singly (typically through orthonormal basis functions), while in the outerproduct model each component of the input pattern multiplies the entire pattern vector. It might induce the same set of additional functionalities for each and every node in the input pattern space. Those two FLN net architecture are shown in Figure 4a and 4b.

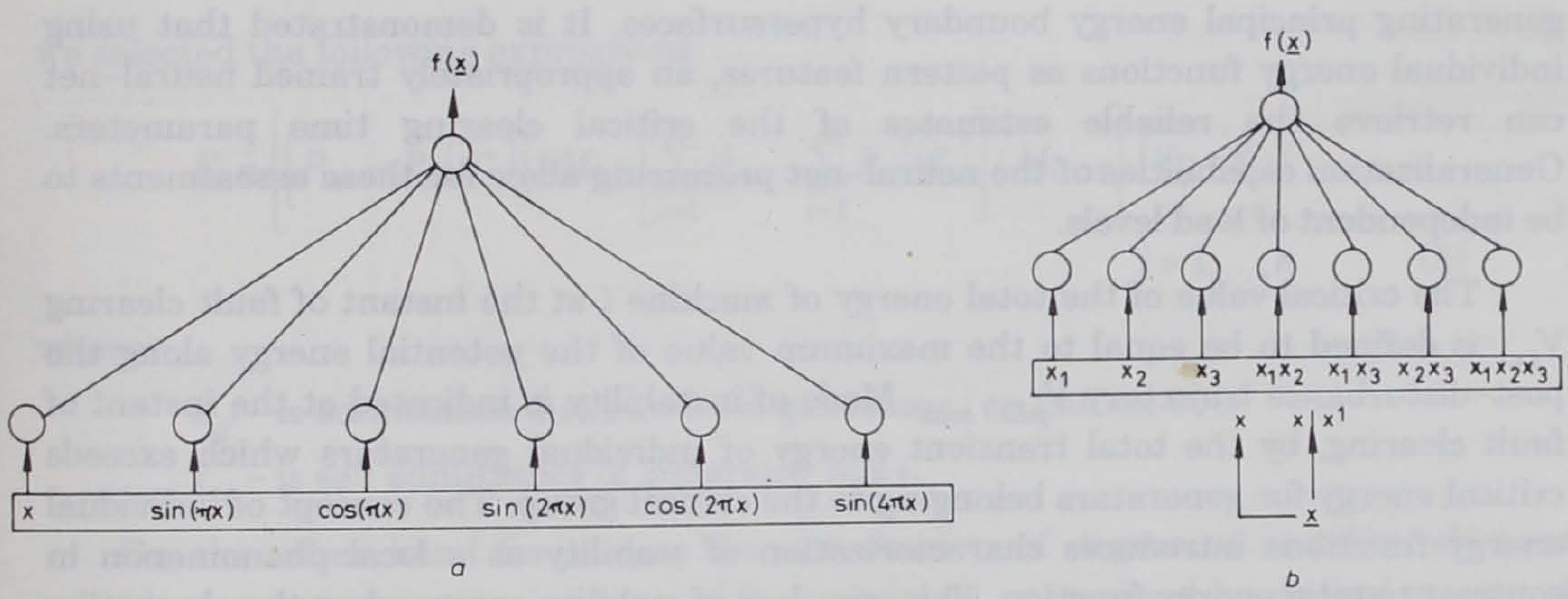

Figure 4. a) The functional expansion model,
b) the outerproduct model of the Functional Link Net architecture

Use of the FLN-net "flat" architecture with no hidden layers increases learning rates and simplifies the learning algorithms.

The basic characteristics of ANN architectures for supervised learning are: layered network, linear operation between layers, nonlinear processing only at nodes, no interaction among nodes in the same layer, iterative convergence to least mean square error representation, processing of binary and analog data.

However, neural-nets are characterized by some inherent shortcomings. The input features for characterization of the phenomena which is being solved must be properly selected to describe a given problem. Backpropagation algorithm doesn' t scale well, the algorithm goes slowly and a criterion how to select the optimum number of hidden layers and the optimum number of nodes in the hidden layers should be developed. The choice of good step parameters often involves a process of trial and error and there is still lack of evidence that the steepest descent algorithm will not converge to the local minimum.

The investigations of artificial neural networks have covered a large number of topics in interpretation, diagnostics, forecasting, predictive monitoring, control and a variety of other tasks [1,3–13,15,16,18–24].

2. NEURAL–NET BASED UNSTABLE MACHINE IDENTIFICATION USING INDIVIDUAL ENERGY FUNCTIONS

In this section a new method for unstable machine identification in power system transient stability studies is presented. It is based on the use of supervised learning neural–net technology, and the adaptive pattern recognition concept. The identification of the mode of instability plays the essential role in the process of generating principal energy boundary hypersurfaces. It is demonstrated that using individual energy functions as pattern features, an appropriately trained neural–net can retrieve the reliable estimates of the critical clearing time parameters. Generalization capabilities of the neural–net processing allow for these assessments to be independent of load levels.

The critical value of the total energy of machine i at the instant of fault clearing $V_{i\,cr}$ is defined to be equal to the maximum value of the potential energy along the post–disturbance trajectory $V_{pEi\,/\,max}$. Mode of instability is indicated at the instant of fault clearing, by the total transient energy of individual generators which exceeds critical energy for generators belonging to the critical group. The concept of individual energy functions introduces characterization of stability as a local phenomenon in contrast to total energy function. This way, loss of stability occurs when the absorption capability of the cutset that encircles the group of machines becomes less than kinetic energy of that group on generators. Relying on local characterization of (in)stability we select individual energy functions at the moment of fault clearing, normalized by critical energy of global energy function as adequate input features which contain in condensed form all relevant information about consequences of given fault on stability of power system.

In order to eliminate necessary numerical integration because of existence of path dependent integrands we propose the following expression for individual energy functions in COI reference frame using the assumption of a linear trajectory in the angle space:

$$V_i^C = \frac{1}{2} M_i \tilde{\omega}_i^{c2} - P_i\left(\theta_i^c - \theta_i^s\right) - \sum_{\substack{j=1 \\ j \neq i}}^{n} C_{ij}^{pf}\left(\theta_i^c - \theta_i^s\right)\left(\cos\theta_{ij}^c - \cos\theta_{ij}^s\right) /$$

$$/\left(\theta_{ij}^c - \theta_{ij}^s\right) + \sum_{\substack{j=1 \\ j \neq i}}^{n} D_{ij}^{pf}\left(\theta_i^c - \theta_i^s\right)\left(\sin\theta_{ij}^c - \sin\theta_{ij}^s\right) / \left(\theta_{ij}^c - \theta_{ij}^s\right) +$$

$$+\frac{M_i}{M_T}\left(\theta_i^c - \theta_i^s\right)\left[\sum_{j=1}^{n} P_j - 2\sum_{j=1}^{n-1}\sum_{k=j+1}^{n} D_{jk}^{pf}\left(\sin\theta_{jk}^c - \sin\theta_{jk}^s\right) / \left(\theta_{jk}^c - \theta_{jk}^s\right)\right] \quad (7)$$

It should be noted that power system's state at fault clearing time (t_c) is calculated analytically using Taylor's series expansion and so individual energy functions at fault clearing time are computed in a straightforward manner.

In order to define features which properly reflect:

- impact of fault on individual generators,
- electrical distance between individual generators and faulted bus,
- changes in network topology,

we selected the following expressions:

$$F_i = \left\{\left[P_{mi} - P_{ei}\left(0^+\right)\right] / M_i - \left[\sum_{i=1}^{n} P_{mi} - \sum_{i=1}^{n} P_{ei}\left(0^+\right)\right] / M_{\mathrm{COI}}\right\}\left(Y_{if} / Y_{ii}\right)$$

$$i = 1, \ldots, n \quad (8)$$

where:

Y_{if} – is admittance distance from generator i to faulted bus,

Y_{ii} – is self admittance of generator bus i.

On the other hand for proper characterization of degree of stability we used individual energy functions at time of fault clearing, normalized by critical energy of global energy function V_{cr}.

$$V_i^{\bullet} = V_i^c / V_{cr} \; ; \quad i = 1, \ldots, n \quad (9)$$

For given fault and fault clearing time (determined by acting of protective devices) we propose two-step procedure for transient security assessment and determination of mode of instability. In the first step, the mode of instability and the CCT parameter are determined using the real-time data. Second step transforms the individual machine energies, for given fault clearing time, into the energy margin (EM) and classifies the system's status as being either stable or unstable. This concept for identification of mode of instability and transient security assessment is summarized in Figure 5.

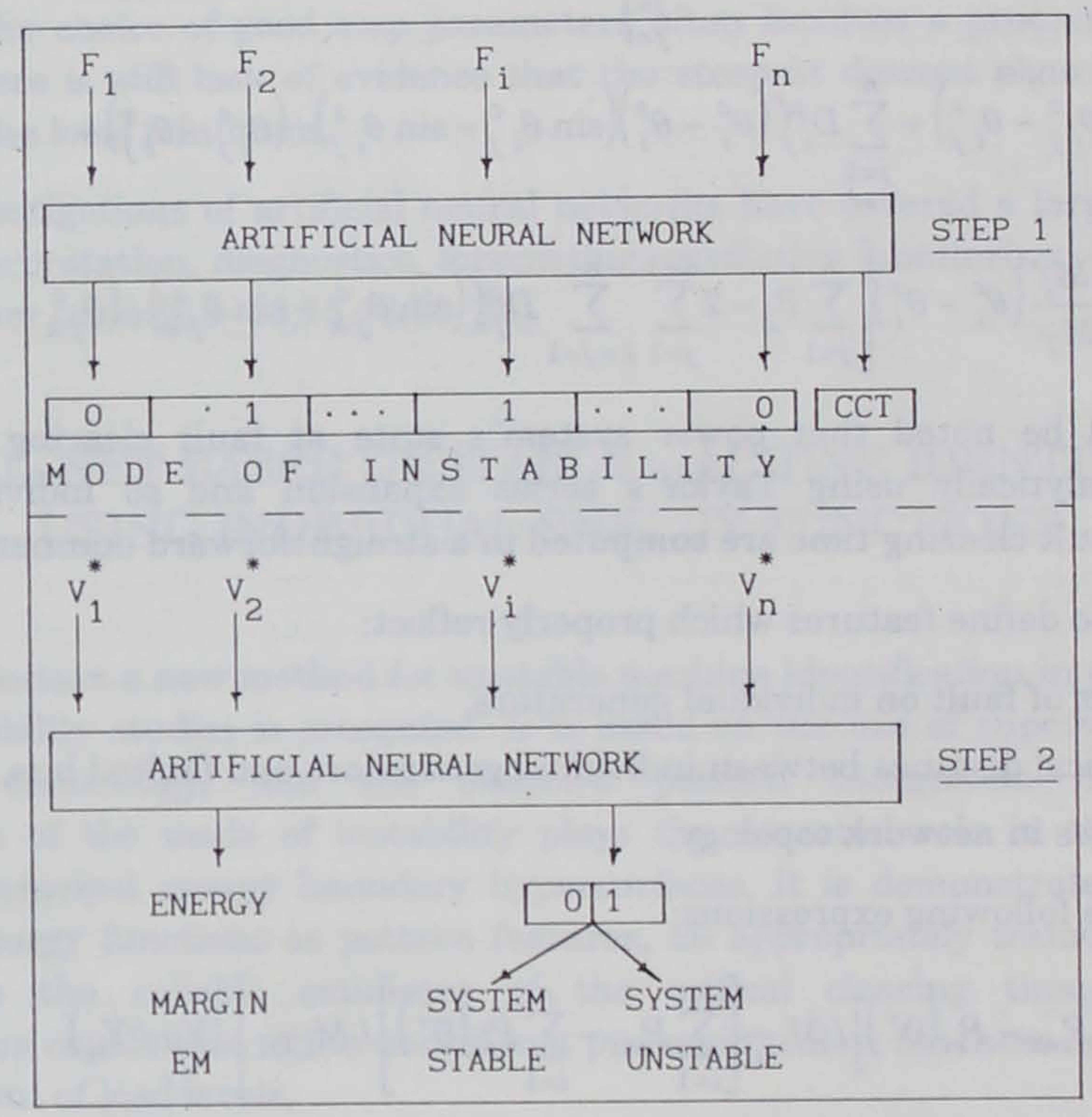

Figure 5. Concept for identification of mode of instability and transient security assessment using individual energy functions

The performance of the ANN for new cases, not presented during the training session is illustrated in Table 1.

It should be observed that the exact prediction of the mode of instability is achieved by ANN even in the case when actual mode of instability changes with the change of load level.

The estimated critical clearing time agrees with the value obtained by numerical integration procedure.

The quality of the ANN based estimation of the energy margin reveals the high generalization power of distributed supervised learning systems.

Advantages of the proposed approach come from the parallelism which is inherent to this method and which provides simple and faster solution to the unstable machine identification and transient security assessment problem. During consulting phase neural–net retrieves mode of instability, energy margin and critical clearing time with order of magnitude more speed than the classical numerical integration method. The speed of execution is an essential requirement of real–time dynamic security assessment schemes.

Table 1. The comparison of actual and estimated CCT, energy margin and mode of instability

Load level (p.u)	Actual CCT (s)	ANN CCT (s)	TEF Method CCT (s)	Actual Mode of Insta-bility	ANN Predict. of MOI	Actual Energy Margin	ANN Energy Margin
FAULTED BUS-35 (FAULT CLEARING WITHOUT LINE SWITCHING)							
0.95	0.28	0.27	0.281	G1-G9	G1-G9	-0.27	-0.31
0.85	0.32	0.32	0.318	G1-G9	G1-G9	+0.06	+0.06
0.75	0.37	0.37	0.358	G1-G9	G1-G9	+0.31	+0.30
0.65	0.41	0.41	0.392	G6	G6	+0.46	+0.47
0.55	0.46	0.45	0.447	G6	G6	+0.63	+0.62

Load level (p.u)	Actual CCT (s)	ANN CCT (s)	TEF Method CCT (s)	Actual Mode of Insta-bility	ANN Predict. of MOI	Actual Energy Margin	ANN Energy Margin
FAULTED LINE 4-14 (FAULT CLEARING WITH LINE SWITCHING)							
0.95	0.26	0.25	0.248	G1-G9	G1-G9	-0.11	-0.08
0.85	0.30	0.31	0.298	G1-G9	G1-G9	+0.25	+0.27
0.75	0.35	0.35	0.351	G1-G9	G1-G9	+0.47	+0.46
0.65	0.38	0.38	0.398	G9	G9	+0.42	+0.41
0.55	0.35	0.37	0.369	G9	G9	+0.56	+0.55

3. ARTIFICIAL NEURAL NETWORK BASED CALCULATION OF GENERATOR-SHEDDING REQUIREMENTS IN POWER SYSTEM EMERGENCY CONTROL

This section presents an application of artificial neural networks in support of a decision-making process of power system operators directed towards fast stabilization of multi-machine systems in emergency control situations. The proposed approach considers generator shedding as the most effective discrete supplementary control for improvement of dynamic performance of faulted power systems and preventing instabilities. Learning capabilities of artificial neural networks are used to establish complex mappings between fault information and the amount of generation to be shed suggesting it as the control signal to the power system operator. Generalization capabilities of ANN-s allow for control decisions to be independent of operating conditions.

We propose an emergency control system based on the use of associated memories. Its schematic diagram is shown in Figure 6.

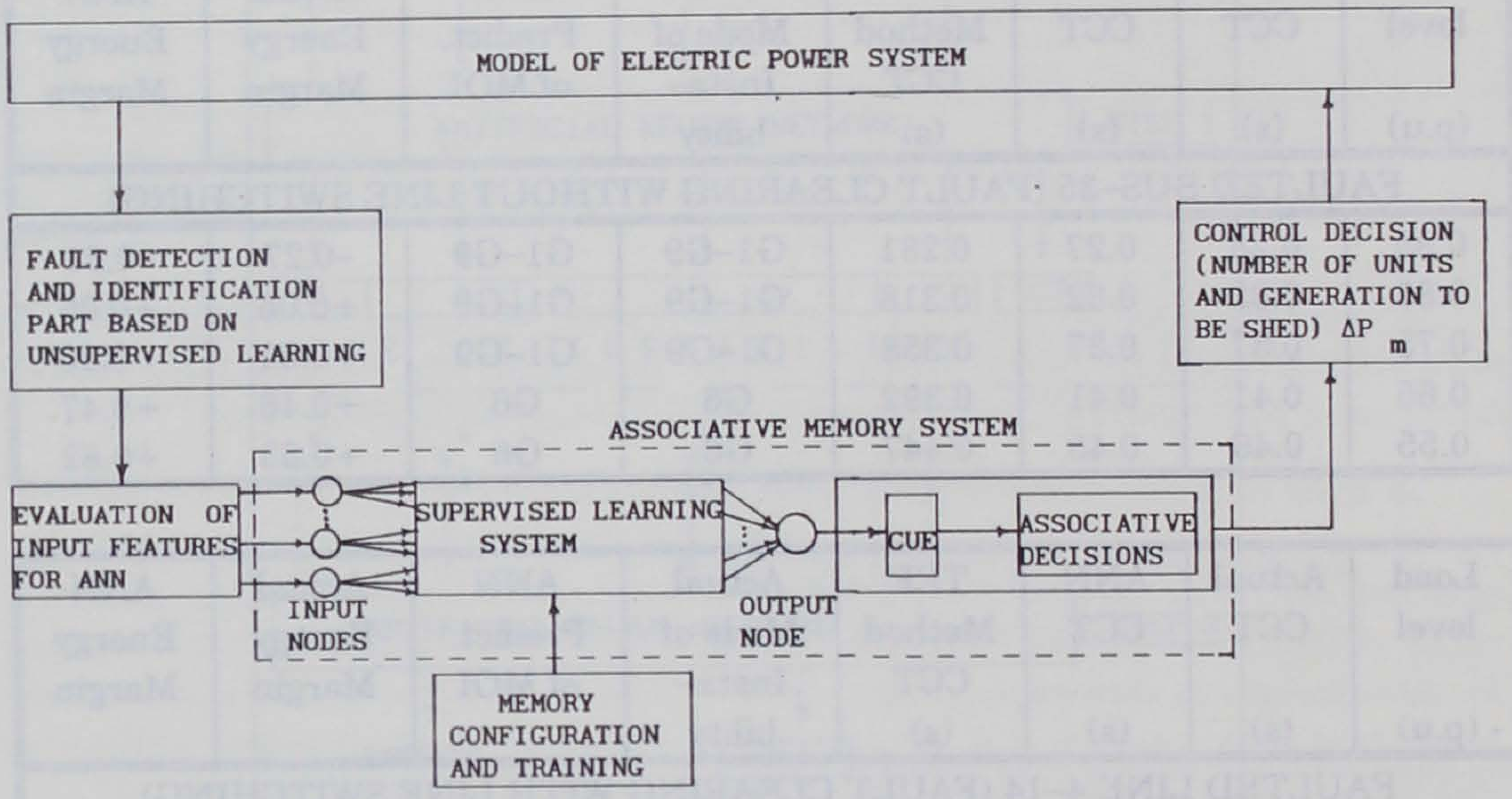

Figure 6. The use of associative memory system for emergency control (AMEC)

The role of fault detection and identification unit (FDI) is to measure the electrical output powers P_{fi} of generators ($i=1,...,n$) and mechanical inputs P_{mi} during a fault and to identify type and location of fault. This information together with the information about topological observability and network connectivity (available from state estimator) is used to calculate input features for a neural net associate memory system according to (8).

The AMEC system consists of two modules. The first one comprises a supervised learning net trained with multi-pass learning methods. Its inputs and outputs (targets) are defined in terms of F_i-coefficients and shed generation, respectively. As the result of learning process a unique set of weights and thresholds is established on the basis of presented data collected under various operating conditions, fault types and network (power) topologies. During a consulting phase, trained net is able to synthesize appropriate emergency control measures, i.e., amounts of shed generation corresponding to new and previously "unseen" circumstances. It should be noticed that the character of the learned map is "analog-to-analog". The nature of the problem dictates quantization of estimated control signals so that shed generation amounts become practically feasible.

The quantization is carried out according to nominal apparent power and number of generator units in power stations which are selected for generator shedding. Then the associate decisions or actions are related to quantization intervals. This is the task of a second module, where the output of a supervised learning system serves as a cue for the associative decision retrieval. If the o:tput node of a supervised network should cause an associated control action to be activated, an message such as "shed 2 units in power station A with mechanical power of 250 MVA" may be recalled providing the output falls within the appropriate quantized interval.

The numerical experiments are carried out on the New England test system [2].

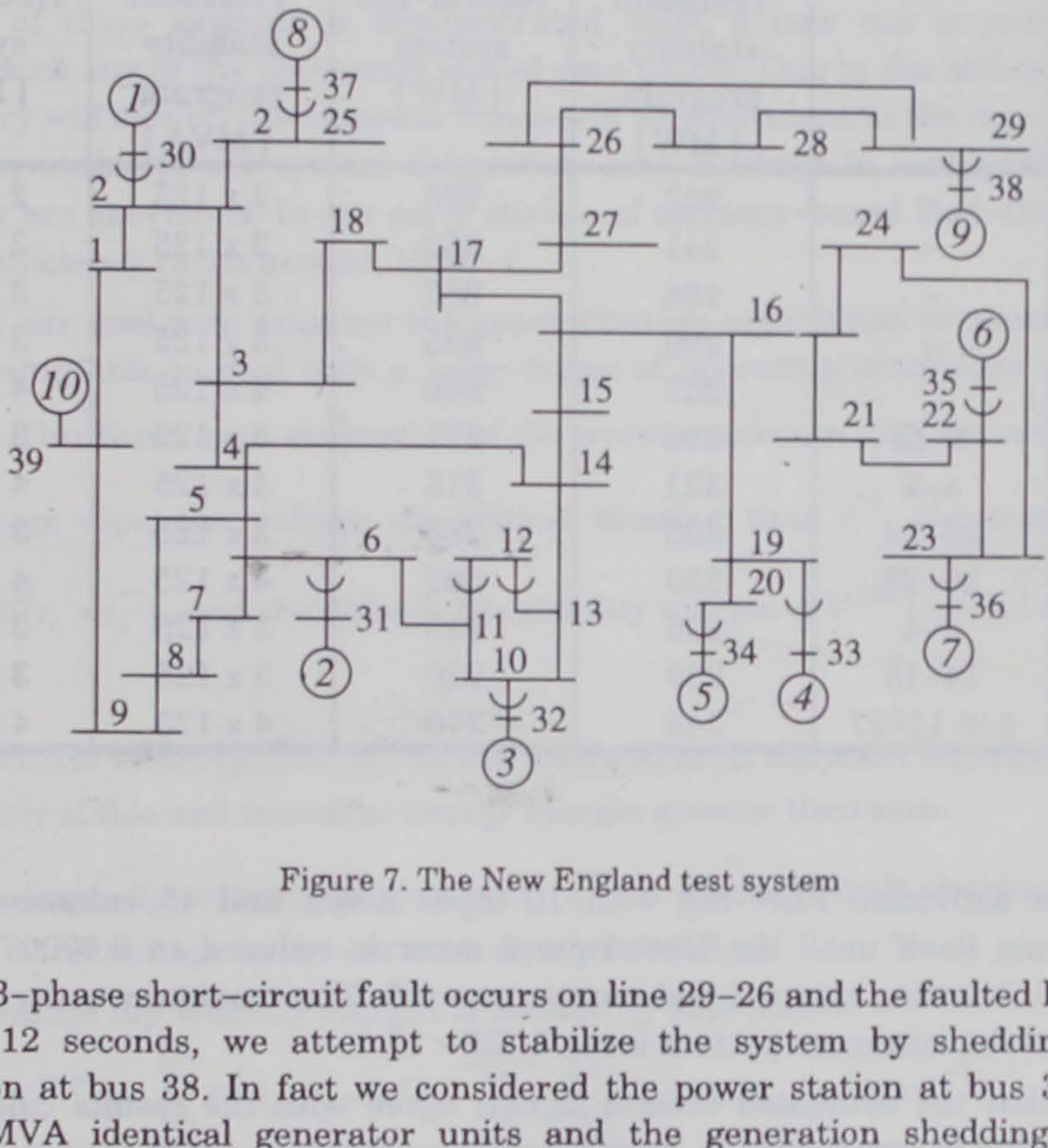

Figure 7. The New England test system

If a 3-phase short-circuit fault occurs on line 29-26 and the faulted line is tripped in $t_f = 0.12$ seconds, we attempt to stabilize the system by shedding a part of generation at bus 38. In fact we considered the power station at bus 38 to contain 8×125 MVA identical generator units and the generation shedding is executed simultaneously with the fault clearing. It should be noted, that fault on line 29-26 with fault clearing policy of isolating fault by tripping the faulted line, causes single mode of instability (generator 9 loses synchronism).

Using a transient stability program the minimum amounts of shed generation are determined necessary to prevent loss of synchronism.

The performance of the neural-net system for new cases, not presented in the training session i.e. for load levels 0.55 0.65 0.75 0.85 and 0.95 [p.u] is illustrated in Table 2.

Table 2. Results of the calculation of the required amount of generation to be shed in the power station G9 for a fault at line 29–26 with $t^c = 0.12$ s

Load level [p.u]	Lines out of service	Minimum amount of shed generation required to stabilize the system calculated by		Number of disconnected units needed to stabilize the system calculated by	
		Transient stability program [MW]	Neural–net system [MW]	Transient stability program [MVA]	Neural–net system [MVA]
0.95	–	203	205	2 x 125	2 x 125
0.85	–	241	233	3 x 125	3 x 125
0.75	–	266	267	3 x 125	3 x 125
0.65	–	299	295	3 x 125	3 x 125
0.55	–	357	346	4 x 125	4 x 125
0.75	3–18	256	271	3 x 125	3 x 125
0.65	4–5	321	318	4 x 125	4 x 125
0.65	23–24	305	285	3 x 125	3 x 125
0.85	26–27	339	362	4 x 125	4 x 125
0.85	3–4	236	246	3 x 125	3 x 125
0.95	14–15	239	220	3 x 125	3 x 125
0.75	5–8 17–27	346	370	4 x 125	4 x 125

The joint activation FLN–net with 10 input nodes and 45 enhancement was allowed to train itself until the least square error is reduced to 0.0000785 in 906 iterations with learning rate 0.7 and momentum 0.5. The maximum pattern error is 2.56×10^{-2} and the minimum pattern error 1.735×10^{-5}.

We see that the estimated control signals agree with the results calculated by transient stability program even in cases when some lines are out of service.

4. NEURAL–NET BASED CALCULATION OF VOLTAGE DIPS AT MAXIMUM ANGULAR SWING IN DIRECT TRANSIENT STABILITY ANALYSIS

In this section we report our investigation of the problem of voltage degradation during system transients. We present a novel approach to estimate the amount of the worst transient voltage dip and the instance of its occurrence. This information is used to activate undervoltage protective devices and update network configuration if necessary and provide the input to the conventional transient security assessment (TSA) routine to evaluate asymptotic stability of the post–fault transient behavior. We propose further to store the outcomes of different simulation runs onto the associative memory appropriately designed as a feedforward neural-net system. Once the "correctness" of the memory has been verified it serves as a fast and reliable estimator of transient voltage characteristics and can be used as a building block in a memory-based design of TSA package for use in real-time conditions.

A parallel hetero-associative memory can be realized using the architecture of a feedforward neural-net system. Stored data can be always retrieved upon the presentation of a cue (input to the neural-net system). More interesting and useful capability of these systems is demonstrated when a new cue is presented, which doesn' t match any of the previously stored data points. Due to the ability to generalize the memory will exhibit the outcome which will be equivalent to the one obtained after running an entire power system simulation case. Savings in computation time and complexity are enormous. In our early studies of memory-based load-flow analysis we observed efficiency ratios around 1000 : 1.

Here, our goal is to examine the generalization capabilities of neural-nets in the scope of being able to deal with a large range of operating conditions with different load levels. Our focus is on estimation of the worst maximum angular swings $\underline{\theta}_{\max}$, the worst voltage dips, the voltage dip critical clearing time t_c^{**}, the transient energy margin $\Delta V(t_c = t_c^{**})$, and the voltage dip stability margin $\Delta V^{\mathrm{DIP}}(t_c = t_c^{*})$ using neural-nets.

The critical clearing time (t_c^{*}) is the maximal fault duration for which the system is transiently stable and transient energy margin greater then zero.

The voltage dip critical clearing time (t_c^{**}) is maximal fault clearing time beyond which the worst voltage in the network dips below 0.8 p.u.

The voltage dip stability margin is defined by expression:

$$\Delta V^{\mathrm{DIP}} = -\sum_{i=1}^{NG} P_i\left(\theta_{\max_i} - \theta_i^{c}\right) - \sum_{i=1}^{NG-1}\sum_{j=i+1}^{NG}\Bigg[C_{ij}\left(\cos\theta_{\max_{ij}} - \cos\theta_{ij}^{c}\right) - \frac{\theta_{\max_i} + \theta_{\max_j} - \theta_i^{c} - \theta_j^{c}}{\theta_{\max_{ij}} - \theta_{ij}^{c}} D_{ij}\left(\sin\theta_{\max_{ij}} - \sin\theta_{ij}^{c}\right)\Bigg] - \frac{1}{2}M_{eq}\tilde{\omega}_{eq}^{c^2} \qquad (10)$$

The voltage dip stability margin is introduced to indicate how far is the system from the critical voltage value below which some load elements will trip. Physically, when the fault clearing time has lasted $t_c > t_c^{**}$ then $\Delta V^{\mathrm{DIP}} < 0$ and network bus voltage magnitudes will dip beyond acceptable level of 0.8 p.u.

In other words we provide a set (pattern) of system description parameters as input to a neural-net and the net returns an estimate of $\theta_{9\,\max}$, t_c^{**}, $\Delta V\left(t_c^{**}\right)$, t_c^{*}, $\Delta V^{\mathrm{DIP}}\left(t_c^{*}\right)$.

The neural-net used in this study consists of three layers, consisting of the input layer with 20 units, one hidden layer with 15 units and a 5 units in the output layer.

Schematically, this concept is illustrated in Figure 8.

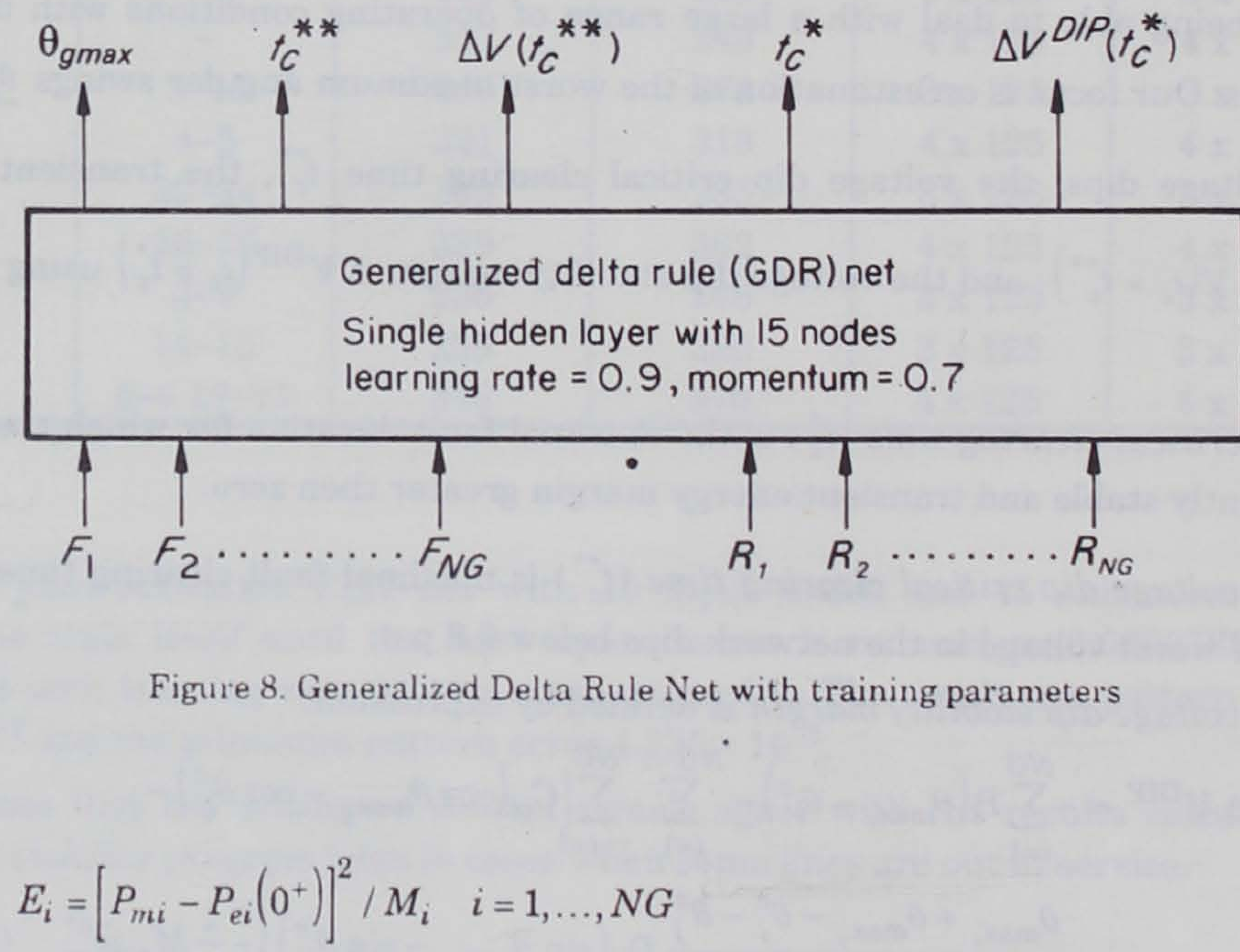

Figure 8. Generalized Delta Rule Net with training parameters

where:

$$E_i = \left[P_{mi} - P_{ei}\left(0^{+}\right)\right]^2 / M_i \quad i = 1,\ldots,NG \tag{11}$$

The performance of the neural-net system for new cases, not presented during the training session i.e. for load levels 0.85 and 0.55 [p.u] is illustrated in Table 3.

In following we display the results of quick prediction of voltage dip stability margin (ΔV^{DIP}) for different fault clearing times (t_c), in order to evaluate the quality of our proposed system in comparison with time-domain simulations. The results are shown in Figure 9.

Table 3. The comparison of actual values (calculated by time domain simulations -TD) and estimated values (calculated by neural-net -NNET) for cases not presented to neural-net during training phase

LOAD LEVEL [p.u]	METHOD	$\theta_{9\,max}$ [degree]	t_c^{**} [s]	$\Delta V(t_c^{**})$ [p.u]	t_c^{*} [s]	$\Delta V^{DIP}(t_c^{*})$ [p.u]
0.85	TD	89.6	0.115	0.81	0.140	-1.04
	NNET	89.8	0.117	0.83	0.142	-1.08
0.55	TD	88.4	0.090	0.61	0.110	-0.68
	NNET	88.5	0.089	0.62	0.109	-0.67

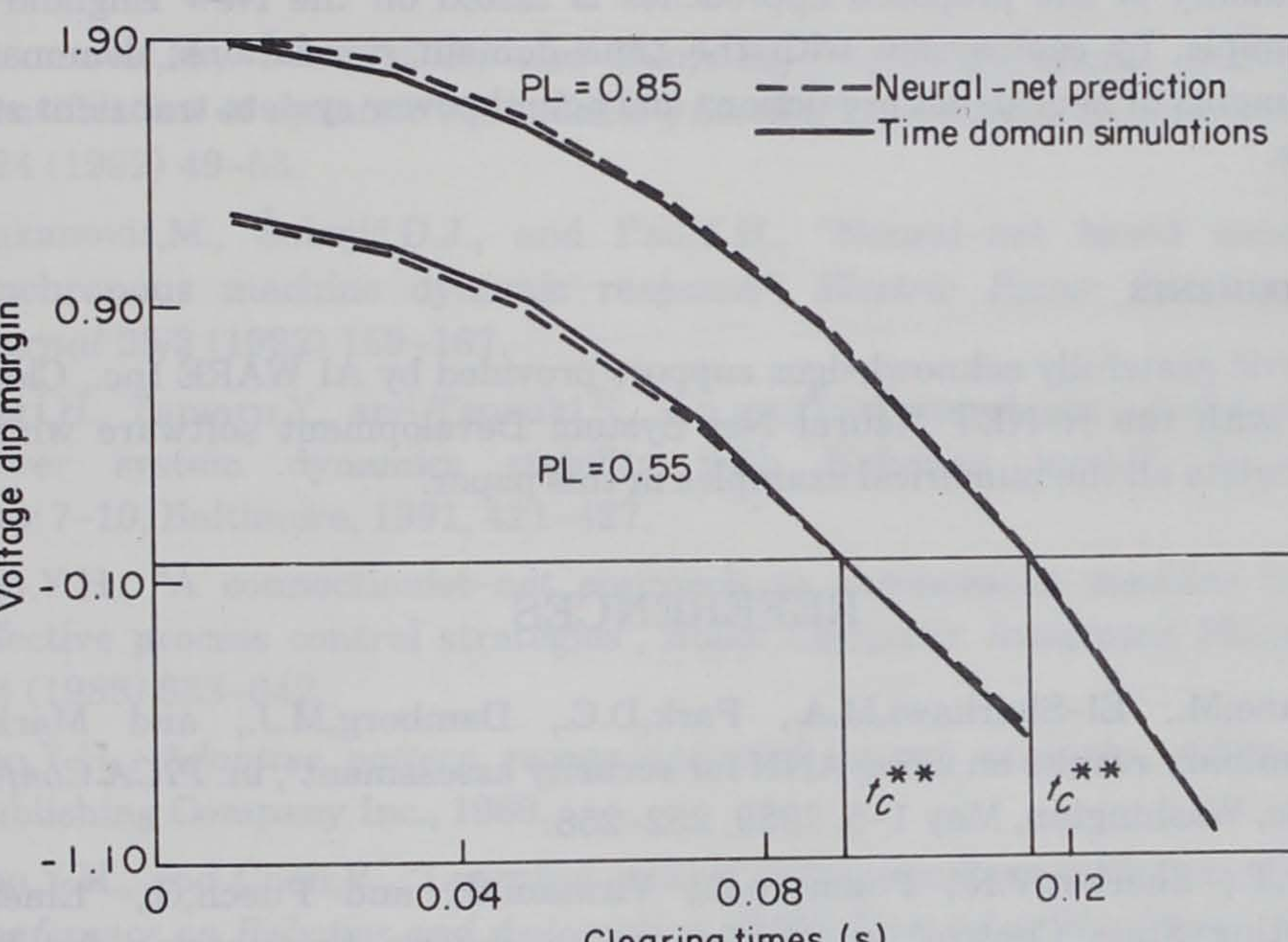

Figure 9. Comparison of voltage dip stability margins (ΔV^{DIP}), obtained by time domain simulations and calculated by neural-net

The quality of the ANN based estimation of the voltage dip parameters reveals the high generalization capability of distributed supervised learning systems.

5. CONCLUSIONS

Artificial neural networks have been proven to be a powerful tool for building the unconventional space transformations such as the one from individual energy functions into the space of essential parameters for stability / instability characterization such as energy margin, critical clearing time and a mode of instability. The present approach performs successfully even in cases when actual mode of instability changes with total power system load level change.

The associative memory system implemented on the computational platform of artificial neural networks is proposed for the fast determination of generator-shedding requirements in power systems. The critical amount of generator-shedding required to prevent the loss of synchronism is determined using the Functional Link Net architecture within the supervised learning process. The complex mappings between fault information and amount of generation to be shed is efficiently learned by neural-nets which are able to suggest the control action after appropriate training.

A new concept for an evaluation of voltage dips at maximum angular swings has been presented suitable for treatment of large disturbances in direct analysis of transient stability.

The validity of the proposed approaches is tested on the New England power system example, by comparison with the time-domain simulations, demonstrating close agreements of neural-net predictions and actual power system transient stability parameters.

ACKNOWLEDGMENTS

M. Đukanović gratefully acknowledges support provided by AI WARE Inc., Cleveland, OH, USA, with the N-NET Neural-Net System Development software which was used to calculate all the numerical examples in this paper.

REFERENCES

[1] Aggoune,M., El-Sharkawi,M.A., Park,D.C., Damborg,M.J., and Marks,R.J., "Preliminary results on using ANN for security assessment", in: *PICA Conference*, Seattle, Washington, May 1-5, 1989, 252-258.

[2] Athay,T., Sherket,V.R., Podmore,R., Virmani,S., and Puech,C., "Emergency Operating State Control" in: *Conference on System Engineering for Power - Section IV*. Davos, Switzerland, Sept. 1979. Also in: U.S. Dept. of Energy Publication No. CONF - 7900904 PL, 1980.

[3] Dillon,T.S., "Artificial Neural Network Applications to Power Systems and their Relationship to Symbolic Methods", *Electrical Power and Energy Systems* 13/2 April (1991) 66-72.

[4] Ebron,S., "Neural network application for data interpretation and diagnostic analysis", in: *Proc. of American Power Conference*, Chicago, April, 1989, 73-78..

[5] El-Sharkawi,M.A., and Marks II,R.J., "Artificial Neural Networks as Operation Aid for On-line Static Security Assessment of power Systems", in: *PSCC*, Graz, Austria, August 19-24, 1990, 895-901.

[6] Chow,M-Y, and Thomas,R.J., "A Neural Network Synchronous Machine Model", in: *IEEE International Symposium on Circuits and Systems*, Portland, Oregon, May 8-11, 1989, 495-498.

[7] Đukanović,M., Šobajić,D.J., and Pao,Y.H., "Neural-net Based Unstable Machine Identification Using Individual Energy Functions", *Electrical Power and Energy Systems* 13/5 Oct. (1991) 255-262.

[8] Đukanović,M., Šobajić,D.J., and Pao,Y.H., "Artificial neural network based calculation of generator-shedding requirements in power systems", in: *IEE Proceedings, Part C, Generation, Transmission and Distribution*, 139/5, Sep. 1992, 427-436.

[9] Đukanović,M., Šobajić,D.J., and Pao,Y.H., "Neural-net based calculation of voltage dips at maximum angular swing in direct transient stability analysis", *International Journal of Electrical Power and Energy Systems* 14/5 October (1992) 341-350.

[10] Đukanović,M., Šobajić,D.J., and Pao,Y.H., "Artificial neural network based identification of dynamic equivalents", *Electric Power Systems Research Journal*, 1/24 (1992) 49-53.

[11] Đukanović,M., Šobajić,D.J., and Pao,Y.H., "Neural-net based simulation of synchronous machine dynamic response", *Electric Power Systems Research Journal* 25/3 (1992) 159-167.

[12] Mori,H., Tamaru,Y., and Tsuzuki,S., "An artificial neural-net based technique for power system dynamics stability with Kohonen model", in: *PICA' 91*, May 7-10, Baltimore, 1991, 421-427.

[13] Pao,Y.H., "A connectionist-net approach to autonomous machine learning of effective process control strategies", *Robot Computer Integrated Manufacturing* 3/4 (1988) 633-642.

[14] Pao,Y.H., *Adaptive pattern recognition and neural networks*, Addison Wesley Publishing Company Inc., 1989.

[15] Pao,Y.H., and Chen,V., "Learning control with neural networks", in: Proc. *IEEE Conference on Robotics and Automation*, IEEE Computer Soc. Press., Scottsdale, May, 1989, 1448-1453.

[16] Pao,Y.H., and Šobajić,D.J., "Combined Use of Unsupervised and Supervised Learning for Dynamic Security Assessment", in: *PICA' 91*, May 7-10, Baltimore, 1991, 522-527.

[17] Rumelhart,D.E., Hinton,G.E., and Williams,R.J., "Learning internal representation by error propagation in parallel distributed processing", *Explorations in the Microstructures of Cognition, vol 1: Foundations*, MIT Press, 1986, 318-362.

[18] Santoso,N.I., and Tan,O.T., "Neural-net based real-time control of capacitors installed on distribution systems", *IEEE Trans. PWRD* 5/1, (1990) 266-272.

[19] Šobajić,D., "Neural-nets for control of power systems", Ph.D. Thesis, Case Western Reserve University, Cleveland, Ohio, 1988.

[20] Šobajić,D.J., and Pao,Y.H., "Artificial neural-net based security assessment for electric power systems", in: *IEEE PES Winter Meeting* #88WM211-5, 1988, also in: *IEEE Transactions on Power Systems* 4/4 February (1989) 220-228.

[21] Šobajić,D.J. and Pao,Y.H., "Neural-net control in power systems", in: *NSF Workshop on Artificial Neural-Net Methodology in Power System Engineering*, Nat. Sci. Fond., Washington DC, Clemson, SC, April 8-10, 1990, 1-7.

[22] Šobajić,D.J., Pao,Y.H., and Dolce,J.L., "On-line monitoring and diagnosis of power system operating conditions using artificial neural networks", in: *IEEE Int. Symposium of Circuits and Systems*, Portland, OR, May 9-12, 1988.

[23] Thomas,R.J., Sakk,E., Hashemi,K., Ku,B.J., and Chiang,H.H., "On-line security screening using an artificial neural network", in: *IEEE-ISCAS-90*, New Orleans, LA, May 1-3, 1990, 2921-2924.

[24] Weerasooriya,S., El-Sharkawi,M.A., Damborg,M., and Marks II,R.J., "Towards static security assessment of a large-scale power system using neural networks", in: IEE Proc.-C, 139/1, Jan. 1992, 64-70.